ISSN 1068-7998, Russian Aeronautics, 2022, Vol. 65, No. 3, pp. 467–473. © Allerton Press, Inc., 2022.
Russian Text © The Author(s), 2022, published in Izvestiya Vysshikh Uchebnykh Zavedenii. Aviatsionnaya Tekhnika, 2022, No. 3, pp. 29–34.

STRUCTURAL MECHANICS AND STRENGTH OF FLIGHT VEHICLES

Application of the Boundary Element Method to Solving the Plane Elastic Problems

A. F. Garif'yanov[a] **and R. Sh. Gimadiev**[a, *]

[a]*Kazan State Power Engineering University, ul. Krasnosel'skaya 51, Kazan, Tatarstan, 420066 Russia*

**e-mail: gimadievr@mail.ru*

Received April 25, 2022; revised May 31, 2022; accepted September 8, 2022

Abstract—The deformation of the hook of the hook–roller connection and the triangular wedge is investigated in linear formulation based on the method of boundary integral equations—the boundary element method.

DOI: 10.3103/S1068799822030047

Keywords: elasticity, plane problem, boundary element method, hook–roller, wedge.

INTRODUCTION

Numerical methods based on finite differences and finite elements are widely used when computing the stress-strain state of various structures. The boundary-integral equation method (BIEM)—the boundary element method can compete with them in a number of tasks, especially in the case of bodies having complex curvilinear contours and various kinds of cutouts. Due to the use of the BIEM studied in [1–13], additional options appear in aeronautical engineering for the computation of complex-shaped parts [14–20].

This method has considerable advantage as it reduces the dimension of the problem under consideration. If a plane body is considered, then the problem is essentially reduced to solving the boundary equations on a contour, and the strains in a plane body are determined by simple integration.

Further, we study the stress-strain state of a curvilinear planar shape (hook–roller) by means of the BIEM. We also consider the deformation of a triangular wedge for the purpose of testing the computation algorithm.

FUNDAMENTALS OF THE BOUNDARY ELEMENT METHOD

The equilibrium equations of the domain element $\Omega(x_1, x_2)$ in the plane problem of linear theory of elasticity have the form $\partial\sigma_{ij}/\partial x_j - b_j = 0$, $i, j = 1, 2$ or

$$\sigma_{ij,j} - b_j = 0, \quad i, j = 1, 2, \tag{1}$$

where the summation runs over repeated subscripts, $\sigma_{ij,j}$ are the derivatives of the stress in the direction α_j; b_j are the components of the stress due to the weight of the plate element.

As a result of the deformation, the coordinates x_i of the domain points are displaced by a quantity u_i. In a linear setting, small deformations can be expressed by means of the deformation tensor

$$\varepsilon_{ij} = \frac{1}{2}\left(\frac{\partial u_i}{\partial x_j} + \frac{\partial u_j}{\partial x_i}\right) = \left(u_{i,j} + u_{j,i}\right)/2. \tag{2}$$

In the case of an isotropic material, Hooke's law has the form

$$\sigma_{ii} = 2G\left(\varepsilon_{ii} + \nu\varepsilon_{jj}\right)\Big/\left(1-\nu^2\right); \quad \sigma_{ij} = G\varepsilon_{ij}; i \neq j, \tag{3}$$

where $G = E\big/\left[2(1+\nu)\right]$ is the shear modulus, E is the tensile modulus, and ν stands for Poisson's ratio.

The Lame equation of equilibrium with respect to displacements has the following form

$$Gu_{j,kk} + G\,u_{k,kj}\big/(1-2\nu) + b_j = 0, \quad k = 1, 2. \tag{4}$$

The stress boundary conditions are written as

$$P_i = 2u_{k,k}n_i G\nu\Big/(1-2\nu) + \left(u_{i,j} + u_{j,i}\right)n_j G, \tag{5}$$

where $P_i = \sigma_{ji}n_j$ are the stresses on the boundary, n_j are the components of the normal unit vector to the boundary of the body.

Let $\Gamma = \Gamma_1 + \Gamma_2$ be the boundary of the body. We assume that the displacements $u_i = \overline{u}_i$ are given on Γ_1, and the stresses $P_i = \sigma_{ji}n_j = \overline{P}_i$ are given on Γ_2.

If the concentrated stresses applied at a point ξ are independent, then the displacements and stresses can be written as $u_j^* = u_{ij}^*(\xi, x)e_i$, $P_j^* = P_{ij}^*(\xi, x)e_i$, where $u_{ij}^*(\xi, x)$, $P_{ij}^*(\xi, x)$ are, respectively, the displacements and stresses that occur at point x in some domain Ω in the jth direction due to the corresponding concentrated unit stress that acts in the direction of the ith unit vector and is applied at point ξ.

The equation for each ith displacement component at point ξ is written in the following form [11]

$$\begin{aligned} u_i(\xi) = &\int_{\Gamma_1}\left(\overline{u}_j(x) - u_j(x)\right)P_{ij}^*(\xi, x)d\Gamma(x) \\ &+ \int_{\Gamma_2}\left(P_j(x) - \overline{P}_j(x)\right)u_{ij}^*(\xi, x)d\Gamma(x) + \int_{\Omega} b_j(x)u_{ij}^*(\xi, x)d\Omega(x). \end{aligned} \tag{6}$$

Equation (6) is known as the Somigliana identity for the displacement (in the domain Ω). This identity is related to the singular Navier solution

$$G\,u_{j,kk}^* + G\,u_{k,kj}^*\big/(1-2\nu) + \delta(\xi, x)e_j = 0, \quad k = 1, 2, \tag{7}$$

where $\delta(\xi, x)$ is the Dirac delta function, $\delta(\xi, x) = 0$ at $\xi \neq x$, $\delta(\xi, x) = \infty$ at $\xi = x$ and $\int_{\Omega^*} b(x)\delta(\xi, x)d\Omega = b(\xi)$. Equation (7) gives a fundamental solution, from which one can determine $u_{ij}^*(\xi, x)$ for Eq. (6).

From Eq. 6, we obtain a continuous distribution of displacements at any point $\xi \in \Omega$. To obtain the stress state, we differentiate the displacements with respect to the coordinates at point ξ. On substituting the result into Eq. (2) and then into Eq. (1), we get the equation for calculating the stress in the domain $\xi \in \Omega$ [11]

$$\begin{aligned} \sigma_{ij}(\xi) = &\int_{\Gamma_1}\left(\overline{u}_k(x) - u_k(x)\right)P_{ijk}^*(\xi, x)d\Gamma(x) \\ &+ \int_{\Gamma_2}\left(P_k(x) - \overline{P}_k(x)\right)u_{ijk}^*(\xi, x)d\Gamma(x) + \int_{\Omega} b_k(x)u_{ijk}^*(\xi, x)d\Omega(x), \end{aligned} \tag{8}$$

where the tensors u_{ijk}^* and P_{ijk}^* are the displacements and stresses at an arbitrary point r due to the concentrated unit stress applied at point ξ along the k axis. These tensors are defined by the following expressions:

$$u^*_{ijk} = \Big((1-2\nu)\big(r_{,j}\delta_{ki} + r_{,i}\delta_{kj} - r_{,k}\delta_{ij} + 2r_{,i}r_{,j}r_{,k}\big)\Big)\Big/\big(4\pi(1-\nu)r\big);$$

$$P^*_{ijk} = \frac{G}{2\pi(1-\nu)r^2}\left[\begin{array}{c} 2\dfrac{\partial r}{\partial n}\Big((1-2\nu)r_{,k}\delta_{ij} + \nu\big(\delta_{ik}r_{,j} + \delta_{jk}r_{,i}\big) - 4r_{,i}r_{,j}r_{,k}\Big) + \\ +2\nu\big(n_i r_{,j}r_{,k} + n_j r_{,i}r_{,k}\big) - (1-4\nu)n_k\delta_{ij} + \\ +(1-2\nu)\big(2n_k r_{,i}r_{,j} + n_j\delta_{ik} + n_i\delta_{jk}\big) \end{array}\right]. \tag{9}$$

Here n_i, n_j are the direction cosines between the normal to the boundary and the directions i, j; δ_{ij} is the Kronecker delta; $r(\xi, x)$ is the distance between the point ξ, where the stress is applied, and some point x of the domain Ω; $r_{,i}$ are the function derivatives with respect to the coordinates of the x point:

$$r = \big(r_i r_i\big)^{1/2}, \quad r_i = x_i(x) - x_i(\xi), \quad r_{,i} = dr/x_i(x). \tag{10}$$

On the boundary, the function $u_i(\xi)$ in Eq. (6) has a discontinuity and is expressed in the following form

$$c_{ij}(\xi)u_i(\xi) + \int_{\Gamma_1}\Big(u_j(x) - \overline{u}_j(x)\Big)P^*_{ij}(\xi, x)\,d\Gamma(x)$$
$$= \int_{\Gamma_2}\Big(P_j(x) - \overline{P}_j(x)\Big)u^*_{ij}(\xi, x)\,d\Gamma(x) + \int_{\Omega} b_j(x)u^*_{ij}(\xi, x)\,d\Omega(x). \tag{11}$$

If surface forces $b_j(x)$ in Eq. (11) are known, then Eq. (11) defines the relation between displacements and stresses on the boundary of the body. For given boundary conditions $\overline{u}_j(x)$ on Γ_1 and $\overline{P}_j(x)$ on Γ_2, this equation is a boundary-integral equation. Equation (11) is the initial one in the boundary-integral equation method and is used along with the fundamental Navier solution (7) for Eq. (6).

In the case of a plane strain state, Kelvin's solution for the displacement on the boundary has the form

$$u^*_{ij} = -\Big((3-4\nu)\ln(r)\delta_{ij} - r_{,i}r_{,j}\Big)\Big/\big(8\pi(1-\nu)G\big). \tag{12}$$

Further, we consider the application of this method to solving two tasks.

COMPUTATION OF THE DEFORMATION OF A PLANE WEDGE

Let us consider the strain state of an isotropic wedge having the shape of a right triangle. Figure 1 shows the stress diagram.

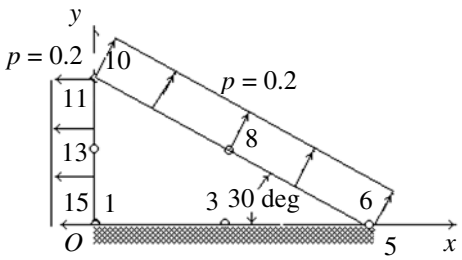

Fig. 1.

In Fig. 1, the length of the hypotenuse of the triangle corresponds to 1 m. The distributed stresses $p = 0.2$ are applied along the normal directions to the hypotenuse and the vertical edge. We chose an adjacent angle of 30 deg so that the total external stress vanishes when projected onto the Ox axis. The triangle contour was split into 12 boundary elements; the angular points are considered twofold. Thus, we have a total of 15 points on the boundary. Using the computation results, we obtained the distribution diagram of the restraint normal forces in the direction of the Oy axis (see Fig. 2).

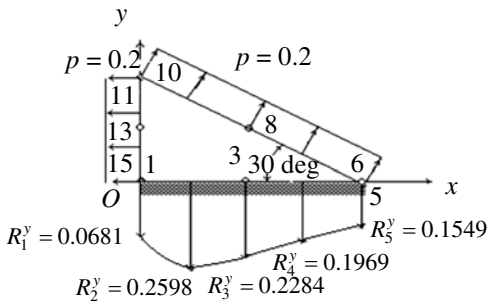

Fig. 2.

The relative error of the integral values of the restraint normal forces and the distributed stress projected onto the Oy axis is of an order of $0.5\,\%$.

COMPUTATION OF THE DEFORMATION OF A HOOK–ROLLER

The action of an external stress causes the hook to bend and shear (Fig. 3). Let r denote the roller radius, and γ—the tilt angle of the upper edge. The hook bends under the action of a force R; as a result, the bending moment becomes $M_{bend} = Rx$, where x is the variable distance between the point of application of the force R and the section being considered with rectangular dimensions h_x and b, where b is the section width.

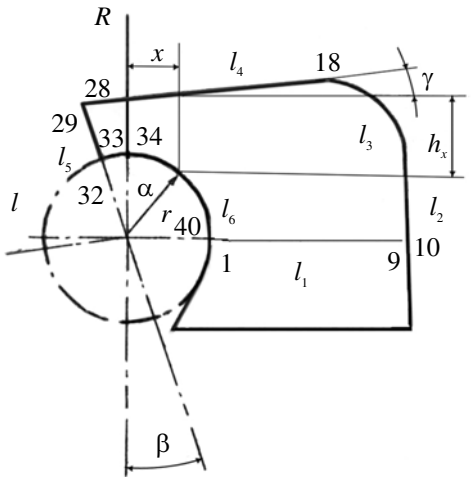

Fig. 3.

Let us consider the stress problem for the hook–roller regarded as an isotropic plate (see Fig. 3). We assume that the roller radius $r = 0.01$ m. The dimensions of the hook are shown in Fig. 3: $l_1 = 0.0226$ m; $l_2 = 0.0166$ m; $l_3 = 0.0157$ m; $l_4 = 0.0274$ m; $l_5 = 0.00667$ m; $l_6 = 0.01902$ m. The angles $\beta = 19$ deg and $\gamma = 0$ deg. The reduced modulus of elasticity of the material $E = 37400$ N/m. The fracture of the material occurs at a stress $\sigma_p = 8600$ N/m. Let the dimensionless values of the stress and the modulus of elasticity be $\bar{\sigma}_p = \sigma_p / [\sigma] = 2$, $\bar{E} = E/[\sigma] = 8.6977$, where $[\sigma] = 4300$ N/m.

We split the contour of the hook into 36 finite boundary elements. There are in total 40 points, taking into account the double angular points (see Fig. 3). Let us assume that the roller acts on the hook with a force $R_{33} = 0.1732$, $R_{34} = 0.1732$, $R_{35} = 0.1732$ along the Oy axis at boundary points 33–35. As a result, the hook bends, and on the line $l_1 = 0.0226$ at points 1–9, there appear the following normal forces: $R_1^Y = -0.481081$; $R_2^Y = -0.264406$; $R_3^Y = -0.134846$; $R_4^Y = -0.052553$; $R_5^Y = -0.002461$; $R_6^Y = 0.030842$; $R_7^Y = 0.061973$; $R_8^Y = 0.084407$; $R_9^Y = 0.258977$.

For the sum of the active forces $R_{33} = 0.1732$, $R_{34} = 0.1732$, $R_{35} = 0.1732$ with respect to point 9 (see Fig. 3), we obtain $\sum M_{act} = 0.0183068$. For the sum of the moments of the normal forces $R_1^Y = -0.481081$; $R_2^Y = -0.264406$; $R_3^Y = -0.134846$; $R_4^Y = -0.052553$; $R_5^Y = -0.002461$; $R_6^Y = 0.030842$; $R_7^Y = 0.061973$; $R_8^Y = 0.084407$; $R_9^Y = 0.258977$ with respect to point 9, we obtain $\sum M_{normal} = 0.018646$.

Thus, the order of the relative error of the moments of these forces is less than $\varepsilon = 1.8\ \%$.

ANALYTICAL METHOD FOR THE COMPUTATION OF THE FRACTURE ANGLE OF THE HOOK–ROLLER

The action of the external stress causes the hook to bend and shear (see Fig. 3). Let r denote the roller radius, and γ —the tilt angle of the upper edge. The hook bends under the action of a force R; as a result, the bending moment becomes $M_{bend} = Rx$, where x is the variable distance between the point of application of the force R and the section being considered. The angle α and the distance x are related to the roller radius r through the dependence $x = r\sin\alpha$. Bending stresses are determined by the formula $\sigma_{bend} = M_{bend}/W$, where $W = bh_x^2/6$ is the resistance moment of the hook section with the rectangular dimensions. Then, according to Fig. 3, the bending stresses satisfy the equation

$$\sigma_{bend} = \frac{6Rr\sin\alpha}{b\left(A - r\cos\alpha + B\sin\alpha\right)^2}, \tag{13}$$

where $A = l\left(\cos\beta + \sin\beta\,\tan\gamma\right)$ and $B = r\tan\gamma$. The denominator in Eq. (13) meets the condition $(A - r\cos\alpha + B\sin\alpha \neq 0)$ for any angle α since $l > r$.

Let us determine the angle α at which the bending stress σ_{bend} that acts on the hook section reaches its maximum value. From the necessary condition of extremum for the function $\sigma_{bend} = \sigma_{bend}(\alpha)$ (namely, $d\sigma_{bend}/d\alpha = 0$), we obtain an equation to determine the angle α:

$$A\cos\alpha - r\left(1 + \sin^2\alpha\right) - B\cos\alpha\sin\alpha = 0. \tag{14}$$

It can be shown that $d\sigma_{bend}^2/d\alpha^2 < 0$. Therefore, the function (13) has a maximum. The angle α, at which the function $\sigma_{bend}(\alpha)$ attains its maximum, can be found from Eq. (14).

Let us write Eq. (14) in approximate form by restricting the expansions of trigonometric functions to two terms ($\sin\alpha = \alpha - \alpha^3/6$ and $\cos\alpha = 1 - \alpha^2/2$):

$$A_3\alpha^3 + A_2\alpha^2 + A_1\alpha + A_0 = 0, \tag{15}$$

where $A_3 = 2B/3$; $A_2 = -(A/2 + r)$; $A_1 = -B$; $A_0 = A - r$.

Equation (15) can be solved by Cardano's formula. Using the solution of Eq. (15) as a first approximation, one can solve Eq. (14) to any required accuracy by iterations.

COMPUTATION OF THE FRACTURE ANGLE OF THE HOOK–ROLLER

The angles and geometry of the hook–roller joint are as follows (see Fig. 3): β = 19 deg, $\gamma = 0$ deg; dimensions: $l = 0.02$ m, $r = 0.01$ m. The approximate solution of Eq. (15) by Cardano's formula gives the maximum value of the angle of bending stress: $\alpha = 38$ deg $30'$. This value can be refined using an iterative method. Finally, we get $\alpha = 41$deg.

According to the results of static fracture tests (Fig. 4), the angle of the fracture onset, at which bending stresses reach their maximum value, was determined as $\alpha = 39$ deg. The fractured piece can be seen in Fig. 4 superposed over a drawing of the hook–roller joint.

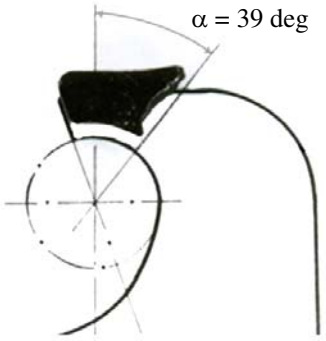

Fig. 4.

CONCLUSIONS

When computing a triangular wedge by the boundary element method, the relative error of the integral values of the restraint normal forces and the distributed stress in projection onto the vertical axis was of the order of 0.5%. The computation of the hook–roller bending by the boundary element method showed good agreement between the moments of active and reactive forces. We suggest an approximate analytic method for the computation of the fracture angle of the hook–roller. The experiment showed a good convergence of the computation results.

REFERENCES

1. Aleksidze, M.A., *Reshenie granichnykh zadach metodom razlozheniya po neortogonal'nym funktsiyam* (Solution of Boundary-Value Problems by the Method of Expansion with Respect to Nonorthogonal Functions), Moscow: Nauka, 1978.
2. Kupradze, V.D., Gegeliya, T.G., Basheleishvili, M.O., and Burchuladze, T.V., *Trekhmernye zadachi matematicheskoi teorii uprugosti i termouprugosti* (The Three-Dimensional Problems of Mathematical Theory of Elasticity and Thermoelasticity), Moscow: Nauka, 1976.

3. Hromadka, T.V. II and Lai, Chentu, *The Complex Variable Boundary Element Method in Engineering Analysis*, New York: Springer Verlag, 1987.
4. *Mekhanika. Novoe v zarubezhnoi nauke* (Mechanics. New Studies in Foreign Science), in 15 vols., Ishlinskii, A.Yu. and Chernyi G.G., Eds., Moscow: Mir, 1978, vol. 15, Boundary Integral Equation Method.
5. *Boundary-Integral Equation Method: Computational Applications in Applied Mechanics*, Cruse, T.A. and Rizzo, F.J., Eds. New York: ASME, 1975.
6. Rizzo, F.J. and Shippy, D.J., An Application of the Correspondence Principle of Linear Viscoelasticity Theory, *SIAM Journal on Applied Mathematics*, 1971, vol. 21, no. 2, pp. 321–330.
7. Rizzo, F.J. and Shippy, D.J., An Advanced Boundary Integral Equation Method for Three-Dimensional Thermoelasticity, *International Journal Numerical Methods Engineering*, 1977, vol. 11, no. 11, pp. 1753–1768.
8. Swedlow, J.L. and Cruse, T.A., Formulation of Boundary-Integral Equations for Three-Dimensional Elasto-Plastic Flow, *International Journal of Solids and Structures*, 1971, vol. 7, no. 12, pp. 1673–1683.
9. Starfiel, A.M., *Boundary Element Methods in Solid Mechanics*, George Allen & Unwin, 1983, 322 p.
10. *Recent Advances in Boundary Element*, Brebbia, C.A., Ed., London: Pentech Press, 1978.
11. Brebbia, C.A., Telles, J.C.F., and Wrobl, L.C., *Boundary Element Techniques. Theory and Applications in Engineering*, Heidelberg: Springer, 1984.
12. Gribov, A.P. and Malakhov, V.G., Calculation of Flexible Plates by the Boundary Element Method, *Trudy mezhdunarodnoi konferentsii posvyashchennoi pamyati zasluzhennogo deyatelya nauki TASSR prof. A.V. Sachenkova "Aktual'nye problemy mekhaniki obolochek"* (Proc. Int. Conf. Dedicated to the Memory of the TASSR Honored Scientist A.V. Sachenkov "Actual Problems of Shell Mechanics"), Kazan: UNIPRESS, 1998, pp. 52–58.
13. Bazhenov, V.G. and Igumnov, L.A., *Metody granichnykh integral'nykh uravnenii i granichnykh elementov* (Methods of Boundary Integral Equations and Boundary Elements), Moscow: Fizmatlit, 2008.
14. Gimadiev, R.Sh., Numerical Simulation of Soft Double-Shell Wing, *Vychislitel'nye Tekhnologii*, IVT SO RAN, Novosibirsk, 1995, vol. 4, no. 11, pp. 51–59.
15. Shabalov, A.V., Khaliulin, V.I., Gimadiev, R.Sh., and Levshonkov, N.V., Modeling the Transformation of Hexactinal Folded Structure, *Izv. Vuz. Av. Tekhnika*, 2019, vol. 62, no. 2, pp. 108–117 [Russian Aeronautics (Engl. Transl.), vol. 62, no. 2, pp. 287–297].
16. Khaliulin, V.I., Savitskii, V.V., Zhukov, A.V., and Gimadiev, R.Sh., Hyperbolic Paraboloid for a Ruled Preform of an X-Fitting: Calculation of Parameters, *Izv. Vuz. Av. Tekhnika*, 2019, vol. 62, no. 3, pp. 4–12 [Russian Aeronautics (Engl. Transl.), vol. 62, no. 3, pp. 353–363].
17. Girfanov, A.M., Ledyankina, O.A., and Gimadiev, R.Sh., Investigation of Modeling Possibility for Lagging of a Helicopter Operating in Transient Flight Regimes, *Izv. Vuz. Av. Tekhnika*, 2019, vol. 62, no. 4, pp. 176–178 [Russian Aeronautics (Engl. Transl.), vol. 62, no. 4, pp. 719–721].
18. Kostin, V.A. and Valitova, N.L., On Improving the Convergence of Calculating the Elastic Properties in a Structure by Means of the Sensitivity Function, *Izv. Vuz. Av. Tekhnika*, 2019, vol. 62, no. 4, pp. 168–171 [Russian Aeronautics (Engl. Transl.), vol. 62, no. 4, pp. 710–714].
19. Gimadiev, R.Sh., Khaliulin, V.I., and Levshonkov, N.V., Calculation of Parameters for Manufacturing the Bearing Surfaces by Pressurization, *Izv. Vuz. Av. Tekhnika*, 2020, vol. 63, no. 2, pp. 3–11 [Russian Aeronautics (Engl. Transl.), vol. 63, no. 2, pp. 177–186].
20. Paimushin, V.N., Firsov, V.A., Shishkin, V.M., Kostin V.A., and Gimadiev, R.Sh., An Investigation into the ASTM E756-05 Test Standard Accuracy on Determining the Damping Properties of Materials in Tension–Compression, *Izv. Vuz. Av. Tekhnika*, 2020, vol. 63, no. 2, pp. 29–37 [Russian Aeronautics (Engl. Transl.), vol. 63, no. 2, pp. 205–213].